



*Cent. Eur. J. Energ. Mater.* 2020, 17(1): 142-163; DOI 10.22211/cejem/119233

Article is available in PDF-format, in colour, at:

[http://www.wydawnictwa.ipo.waw.pl/cejem/Vol-17-Number1-2020/CEJEM\\_01068.pdf](http://www.wydawnictwa.ipo.waw.pl/cejem/Vol-17-Number1-2020/CEJEM_01068.pdf)



Article is available under the Creative Commons Attribution-NonCommercial-NoDerivs 3.0 license CC BY-NC-ND 3.0.

*Research paper*

## Synthesis and Curing of Allyl Urethane NIMMO-THF Copolyether with Three Functional Groups as a Potential Energetic Binder

Xiaochuan Wang<sup>1</sup>, Ping Li<sup>2,\*</sup>, Xianming Lu<sup>3</sup>, Hongchang Mo<sup>3</sup>,  
Minghui Xu<sup>3</sup>, Ning Liu<sup>3</sup>, Yuanjie Shu<sup>3</sup>

<sup>1</sup> *School of Biomedical Sciences and Engineering,  
Guangzhou International Campus, South China University  
of Technology, Guangzhou 510006, China*

<sup>2</sup> *School of Mechanical and Electric Engineering,  
Guangzhou University, Guangzhou 510006, China*

<sup>3</sup> *Xi'an Modern Chemistry Research Institute, Xi'an 710065, China*

\*E-mail: [leeping0521@126.com](mailto:leeping0521@126.com)

**Abstract:** A tri-functional NIMMO-THF copolyether (T-NT) was synthesized by polymerization of 3-nitratomethyl-3-methyloxetane (NIMMO) and tetrahydrofuran (THF) in the presence of trimethylolpropane and catalyzed by  $\text{BF}_3 \cdot \text{OEt}_2$ . The allyl urethane NIMMO-THF copolyether with three functional groups (AUT-NT) was synthesized from tri-functional NIMMO-THF copolyether and allyl isocyanate. The polymer was characterized by FT-IR,  $^1\text{H}$  NMR, and  $^{13}\text{C}$  NMR. Furthermore, an elastomer that was prepared from allyl urethane NIMMO-THF copolyether with three functional groups and trimethylisophthalodinitrile oxide (TINO) had satisfactory mechanical properties and good thermal stability. The elastomer is expected to be used in composite solid propellants and polymer-bonded explosives (PBX).

**Keywords:** energetic binder, copolyether, nitrile oxide, elastomer

## 1 Introduction

There are a lot of polymers with special structures and excellent performance, such as hydroxyl-terminated polybutadiene (HTPB), hydroxyl terminated polyether (HTPE), polyethylene glycol (PEG) and so on [1-6]. In recent years, a new trend has been the replacement of these inert binders by energetic binders such as glycidyl azide polymer (GAP) [7-11] and poly[(3-nitratomethyl)-3-methyloxetane] (polyNIMMO) [12-18], in order to develop advanced rocket propellants and polymer-bonded explosives (PBX). PolyNIMMO is an energetic polymer with high energy output and good compatibility with highly energetic oxidizers. However, its higher  $T_g$  ( $-30\text{ }^\circ\text{C}$ ) and its mechanical properties are not suitable for use as a propellant binder. The preparation of a copolymer of tetrahydrofuran (THF) and NIMMO may provide a rather more suitable energetic propellant binder, although there is energy loss when replacing polyNIMMO with the proposed copolymer [19, 20].

These are telechelic polymers terminated at each end with a hydroxyl functional group, which are usually cross-linked by an isocyanate curing agent to form polyurethanes [21-29]. The polyurethane's three-dimensional network exhibits excellent mechanical properties. However, there are some disadvantages of hydroxyl-terminated polymer and isocyanate systems. The inherent incompatibility of isocyanates with ammonium dinitramide (ADN) and the humidity sensitivity of the curing process demand a new curing system [30-33].

Nitrile oxides are organic compounds which contain the  $-\text{CNO}$  group bound directly to a carbon atom [34-38]. Sterically hindered bifunctional nitrile oxides are stable indefinitely at room temperature. They can be used to crosslink unsaturated polymers. The  $-\text{CNO}$  groups react with  $\text{C}=\text{C}$  bonds to form isoxazolines. Since there are two  $-\text{CNO}$  groups in each trimethylisophthalodinitrile oxide (TINO) molecule, TINO can be used as a room-temperature curing agent for curing unsaturated polymers [39, 40]. Furthermore, since there are three  $\text{C}=\text{C}$  bonds in each allyl urethane NIMMO-THF copolyether molecule and two  $-\text{CNO}$  groups in each TINO molecule, a cross-linked network can be obtained by the curing system, *via* 1,3-dipolar cycloaddition of the nitrile oxide and the  $\text{C}=\text{C}$  group.

In the present study, allyl urethane NIMMO-THF copolyether with three functional groups (AUT-NT) was synthesized *via* the tri-functional NIMMO-THF copolyether and allyl isocyanate. The tri-functional NIMMO-THF copolyether (T-NT) was synthesized by polymerization of NIMMO and THF in the presence of trimethylolpropane (TMP) catalyzed by boron trifluoride

etherate ( $\text{BF}_3 \cdot \text{OEt}_2$ ). The structures of these products were confirmed by FT-IR,  $^1\text{H}$  NMR,  $^{13}\text{C}$  NMR, and their thermal stability was estimated by DSC. The mechanical properties of an isoxazoline elastomer based on AUT-NT and TINO were compared with those of a polyurethane elastomer based on T-NT and hexamethylene diisocyanate (HDI).

## 2 Experimental

### 2.1 Materials

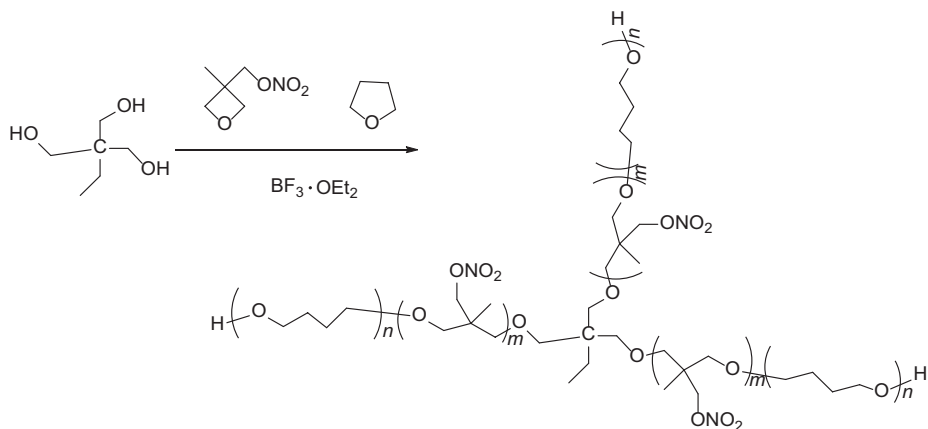
NIMMO was prepared based on a reported method [41].  $\text{BF}_3 \cdot \text{OEt}_2$ , dichloromethane,  $\text{Na}_2\text{CO}_3$ , and  $\text{MgSO}_4$  were obtained from the Xi'an Chemical Reagents Factory (Xi'an, Shaanxi province, China). THF, TMP, and HDI were purchased from J&K Scientific Ltd. (Shanghai, China). Allyl isocyanate was purchased from Energy Chemical (Shanghai, China).

### 2.2 Characterization methods

FTIR spectra were measured with a Bruker Tensor 27 instrument (KBr pellets) with a resolution of  $4\text{ cm}^{-1}$  in the range  $400\text{--}4000\text{ cm}^{-1}$ .  $^1\text{H}$  NMR and  $^{13}\text{C}$  NMR spectra were recorded with a Bruker 500 MHz instrument using  $\text{CDCl}_3$  as solvent. DSC, conducted with a TA Instruments DSC Q1000, was used to thermally characterize the samples using a heating/cooling rate of  $10\text{ }^\circ\text{C}\cdot\text{min}^{-1}$ .

## 2.3 Preparation

### 2.3.1 Synthesis of tri-functional NIMMO-THF copolyether (T-NT)



**Scheme 1** Synthetic route for T-NT

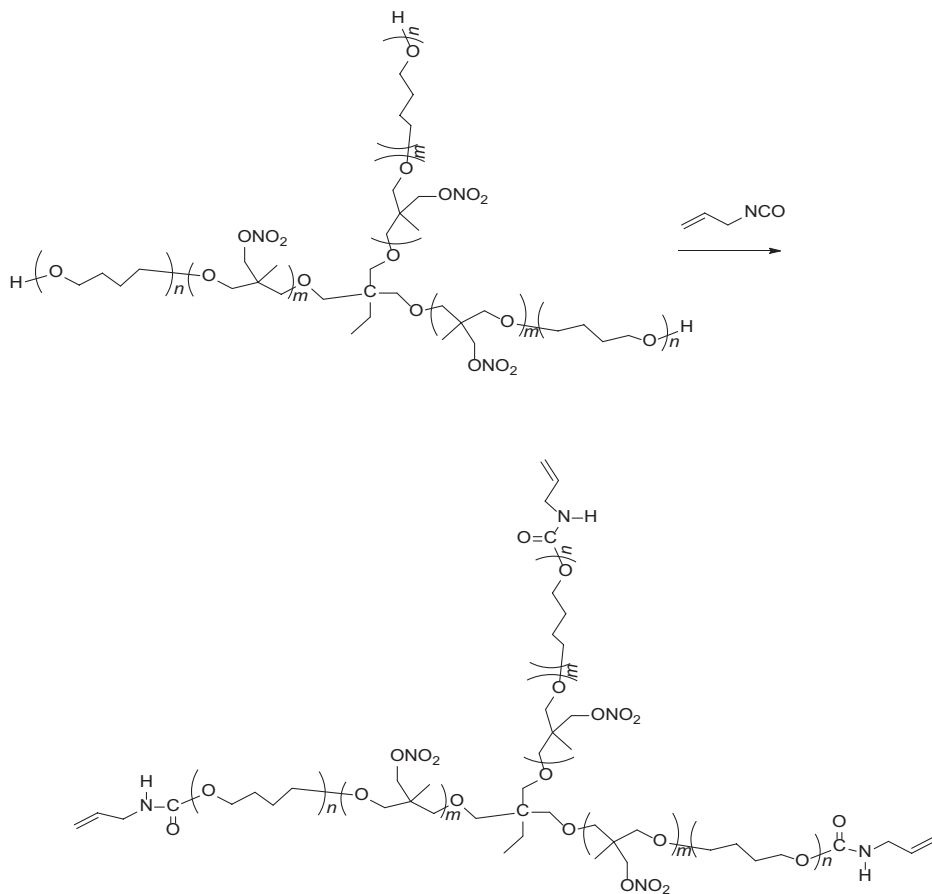
TMP (0.65 g, 0.005 mol),  $\text{BF}_3 \cdot \text{OEt}_2$  (2.1 g, 0.015 mol), and THF (5.4 g, 0.075 mol) were added to a 3-necked round-bottomed flask fitted with a thermometer and stirred for 30 min at 25 °C. NIMMO (11 g, 0.075 mol) was then added dropwise over a period of 2 h. After the addition of the monomers, the reaction was left to react for another 24 h. The reaction mixture was then dissolved in dichloromethane. The reaction was halted by the addition of an aqueous solution of  $\text{Na}_2\text{CO}_3$ . The mixture was separated, the organic layer removed and the  $\text{CH}_2\text{Cl}_2$  evaporated to leave the polymer. The yield of T-NT was 16.87 g (98.9%).

### 2.3.2 Preparation of the polyurethane elastomer based on T-NT and HDI

The polyurethane elastomer based on T-NT and HDI was prepared *via* mixing T-NT and HDI at an NCO/OH ratio of 1.1. A typical synthesis procedure was as follows: T-NT was mixed with HDI and degassed on a rotary evaporator for 30 min. The mixture was then cast into a Teflon<sup>®</sup> mold with a thickness of approximately 2 mm and left to react for 7 days at 65 °C. The polyurethane elastomer obtained was cut into dumbbell-shaped specimens for measurement of the mechanical properties.

### 2.3.3 Synthesis of allyl urethane NIMMO-THF copolyether (AUT-NT)

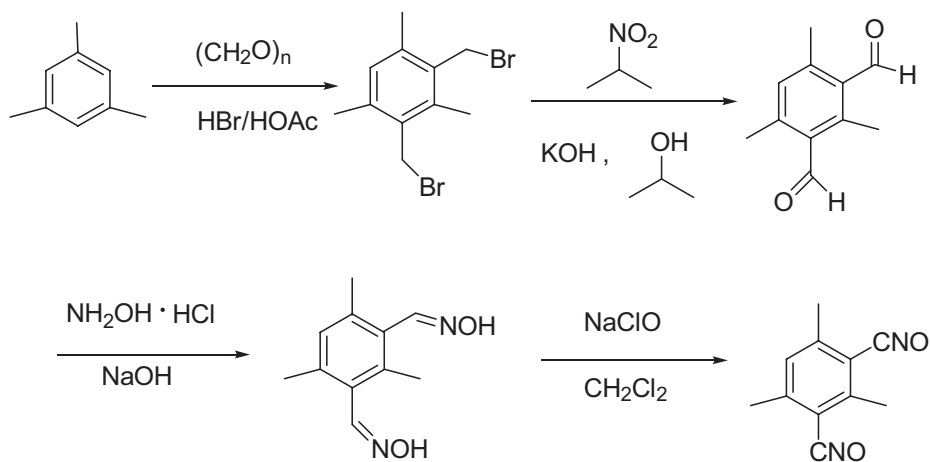
T-NT (16.87 g, 0.01 mol) was added to a 3-necked round-bottomed flask fitted with a thermometer. Allyl isocyanate (1.25 g, 0.015 mol) was added dropwise over a period of 10 min at 50 °C. After the addition of allyl isocyanate, the reaction was left to react for 12 h at 75 °C. Orange AUT-NT (18.12 g, 100%) was obtained (Scheme 2).



**Scheme 2.** Synthetic route for AUT-NT

### 2.3.4 Preparation of an isoxazoline elastomer based on AUT-NT and TINO

The trimethylisophthalodinitrile oxide (TINO) was synthesized in four steps in a total yield of 42%. The schematic synthetic route is shown in Scheme 3. The crude TINO was recrystallized from acetone. An SEM image of TINO (purity of 99% or more) is shown in Figure 1. The crystal morphology of TINO can be observed from the SEM image. It is colorless, crystalline and sparkles in the sunshine.



**Scheme 3.** Synthesis of TINO

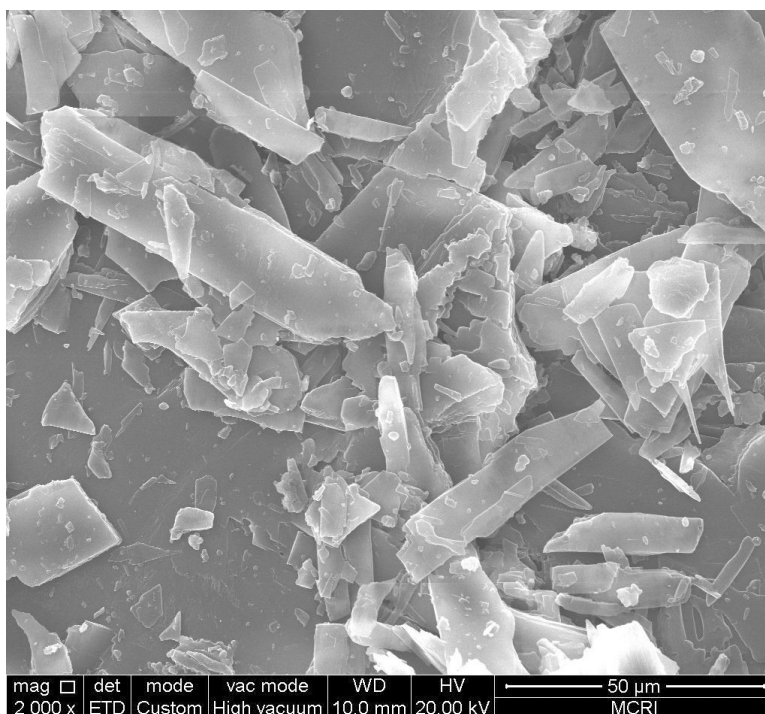


**Figure 1.** The SEM image of TINO cultivated from acetone

The isoxazoline elastomer based on AUT-NT and TINO was prepared *via* mixing TINO and AUT-NT at a CNO/C=C ratio of 1. A typical synthetic procedure (see Figure 2) was as follows: TINO was mixed with  $\text{CH}_2\text{Cl}_2$  to obtain a clear solution. The solution was mixed with AUT-NT for 5 h. The mixture was then cast into a Petri dish mold and left to react for 7 days at 25 °C. The isoxazoline elastomer obtained was cut into dumbbell-shaped specimens for measurement of the mechanical properties.

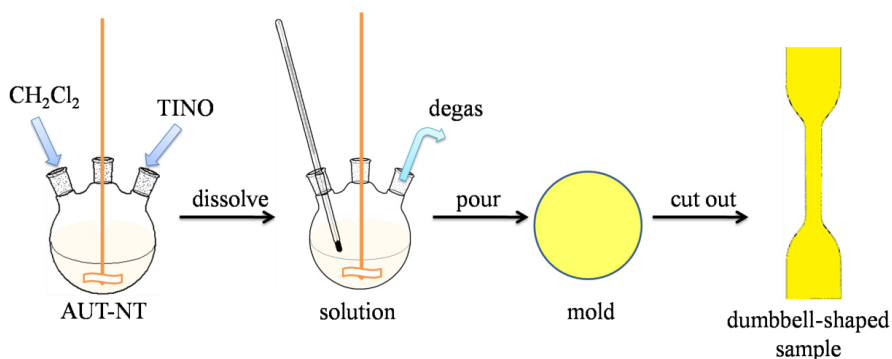


**Figure 2.** The preparation flow chart for the isoxazoline elastomer

### 3 Results and Discussion

#### 3.1 FT-IR spectra of T-NT and AUT-NT

Figure 3 shows the FT-IR spectra of T-NT and AUT-NT. In the FT-IR spectrum of T-NT, the symmetric and unsymmetric stretching vibrations of  $\text{NO}_2$  were observed at  $1630$  and  $1280\text{ cm}^{-1}$ . The observed peak at  $2865\text{ cm}^{-1}$  was attributed to the stretching vibration of C–H. In the FT-IR spectrum of AUT-NT, the stretching vibration of N–H was observed at  $3444\text{ cm}^{-1}$ . The in-plane bending vibration of N–H was observed at  $1518\text{ cm}^{-1}$ . The observed peak at  $1727\text{ cm}^{-1}$  was attributed to the stretching vibration of C=O. Moreover, the other peaks, including  $2865$ ,  $1633$ ,  $1280$  and  $1111\text{ cm}^{-1}$ , are the same as with T-NT.



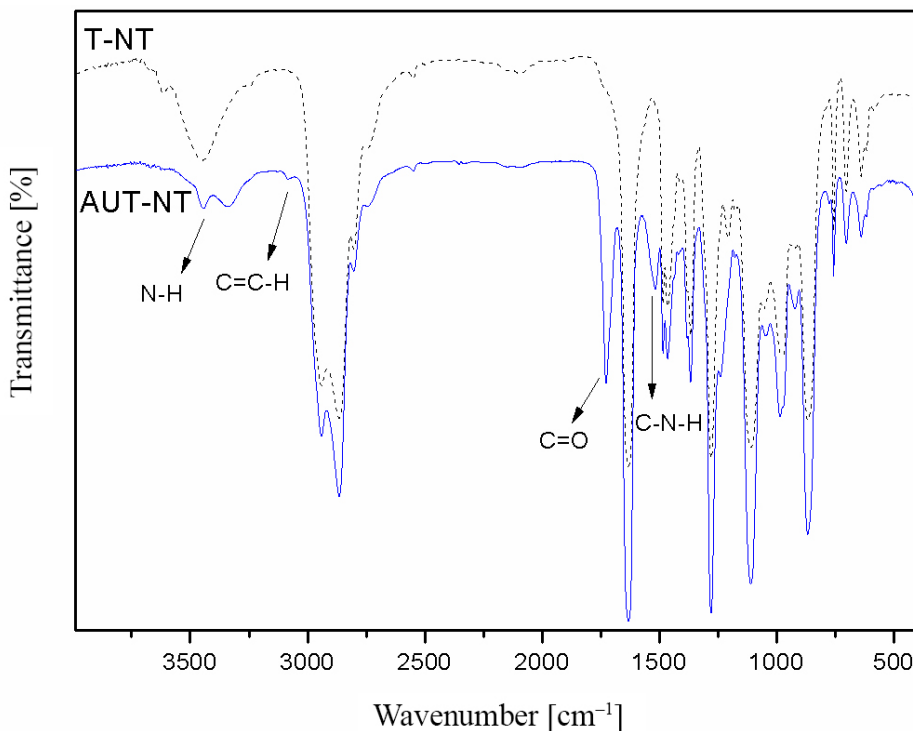


**Figure 3.** FT-IR spectra of T-NT and AUT-NT

### 3.2 NMR spectra of T-NT and AUT-NT

As shown in Figure 4, in the  $^1\text{H}$ NMR spectrum of T-NT the signals observed at 0.96-1.00 ppm were attributed to the methyl protons of the side chain. The signals at 1.50-1.60 ppm were due to the methylene (not adjacent to O atoms) protons of the main chain. The signals at 3.25-3.37 ppm were due to the methylene (adjacent to O atoms) protons of the main chain. The signals at 4.31-4.49 ppm were attributed to the methylene protons of the side chain [42]. In the  $^1\text{H}$  NMR spectrum of AUT-NT, the signals at 5.85, 5.24, 5.13 ppm were due to the alkenyl protons (denoted a, b and c) of the main chain. The signals at 4.01 and 3.80 ppm were due to the methylene protons (denoted d and e) of the main chain.

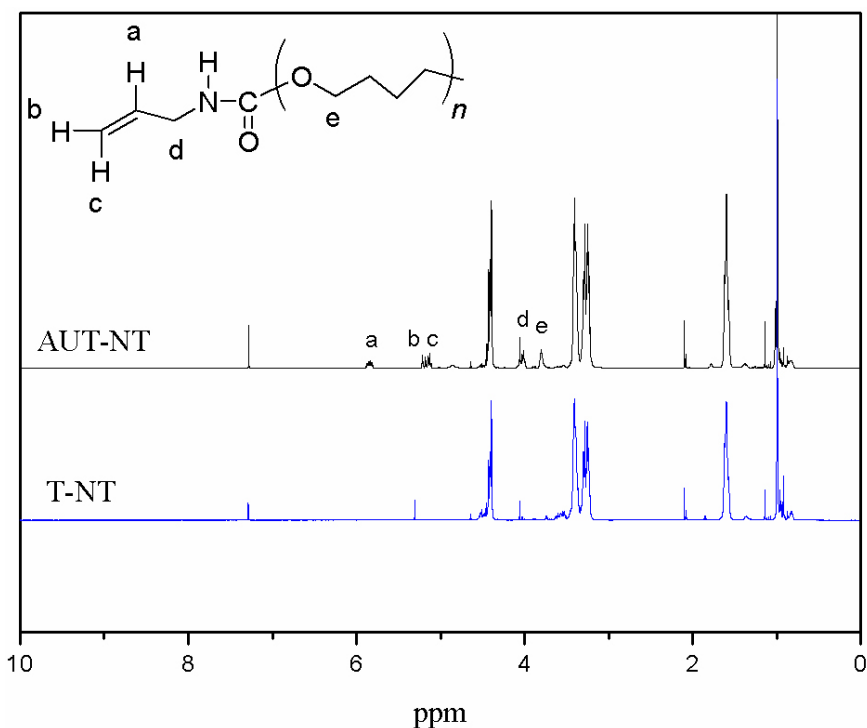


**Figure 4.**  $^1\text{H}$  NMR spectra of T-NT and AUT-NT

The successful reaction was also confirmed by the  $^{13}\text{C}$  NMR spectrum. As shown in Figure 5, the resonances of carbons are similar to those of T-NT. The differences were as follow. The resonances of the alkenyl carbons (denoted c, d) in the main chain appeared at 116.3 and 134.3 ppm. The resonances of the carbonyl carbons (denoted a) in the main chain appeared at 155.9 ppm. The resonances of the methylene carbons (denoted b) in the main chain appeared at 43.5 ppm.

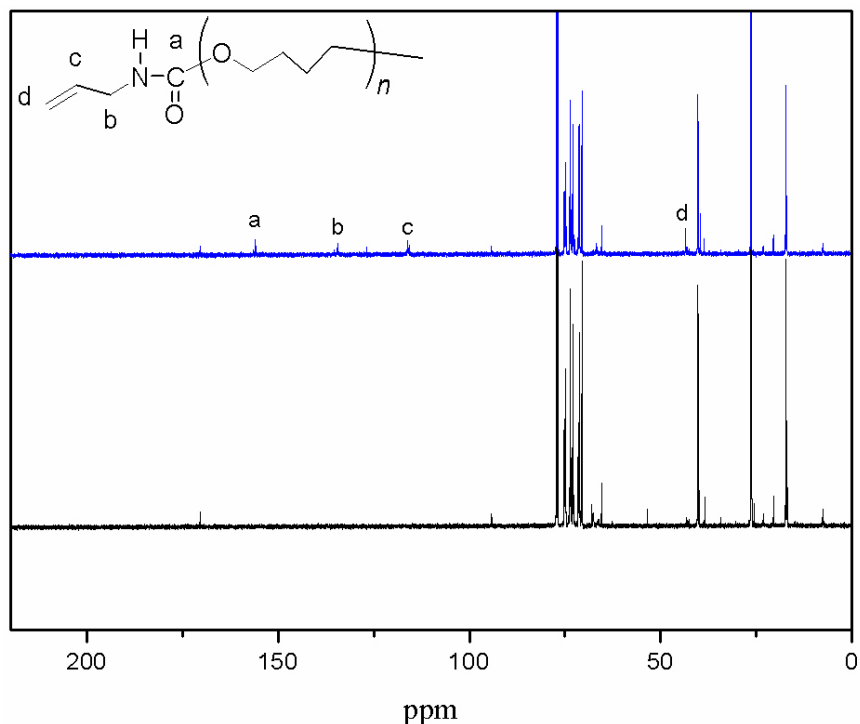


**Figure 5.**  $^{13}\text{C}$  NMR spectra of T-NT and AUT-NT

### 3.3 FT-IR spectra of the blend of T-NT and HDI, polyurethane elastomer and T-NT

FT-IR spectra of the blend of T-NT and HDI, the polyurethane elastomer and T-NT are shown in Figure 6. Comparison of the spectra shows that the disappearance of the strong absorption peak ( $2275\text{ cm}^{-1}$ ) of  $-\text{NCO}$  indicates completion of the reaction. There are three  $-\text{OH}$  groups in each T-NT molecule and two  $-\text{NCO}$  groups in each HDI molecule. The  $-\text{NCO}$  groups of HDI react with the  $-\text{OH}$  groups of AUT-NT to form the polyurethane. As a result, the FT-IR absorption peak of the  $-\text{NCO}$  groups disappeared.

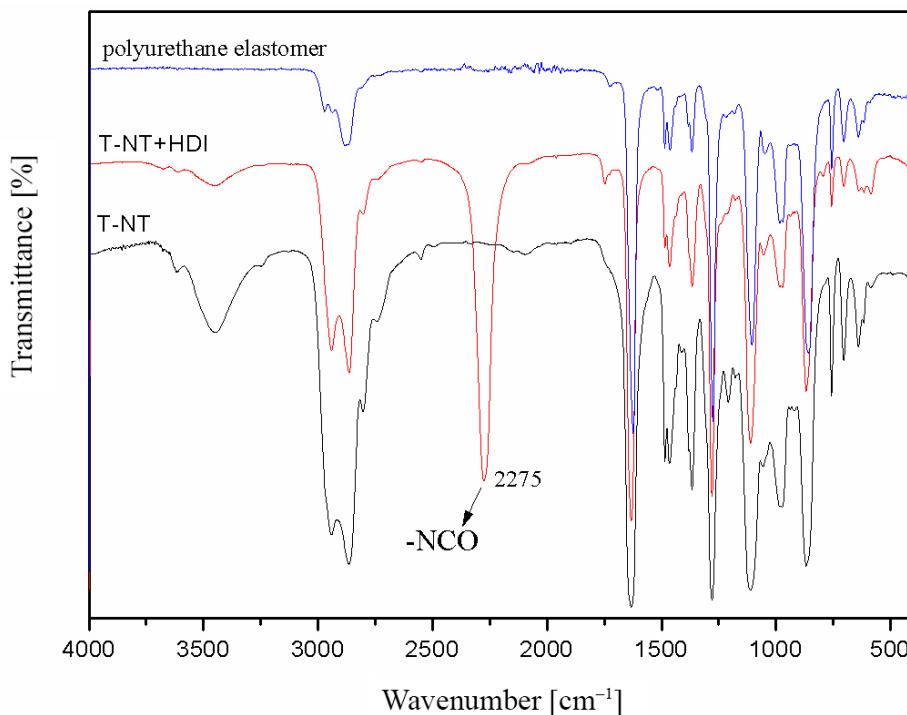


**Figure 6.** FT-IR spectra of the blend of T-NT and HDI, polyurethane elastomer and T-NT

### 3.4 FT-IR spectra of the blend of AUT-NT and TINO, the isoxazoline elastomer and AUT-NT

FT-IR spectra of the blend of AUT-NT and TINO, the isoxazoline elastomer and AUT-NT are shown in Figure 7. Comparison of the spectra shows that the disappearance of the strong absorption peak (2291 cm<sup>-1</sup>) of –CNO indicates completion of the 1,3-dipolar cycloaddition reaction. There are three C=C bonds in each AUT-NT molecule and two –CNO groups in each TINO molecule. The –CNO groups of TINO react with the C=C bonds of AUT-NT to form the isoxazolines. As a result, the FT-IR absorption peak of the –CNO groups disappeared.

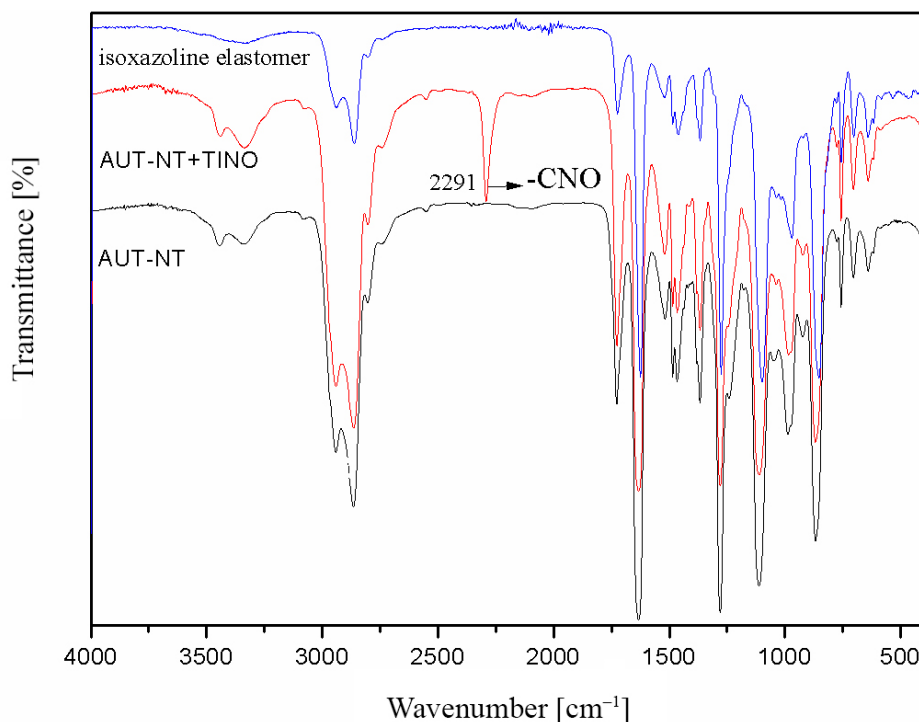


**Figure 7.** FT-IR spectra of the blend of AUT-NT and TINO, isoxazoline elastomer and AUT-NT

### 3.5 The mechanical properties of the isoxazoline elastomer and the polyurethane elastomer

Tensile testing was used to evaluate the ultimate mechanical properties of the polyurethane elastomer based on T-NT and HDI, and the isoxazoline elastomer based on AUT-NT and TINO (Table 1). The tests were performed according Chinese standards GB/T 528-2009 and the test conditions were: dumbbell-shaped specimens at 20 °C with speed of extension 500 mm/min. The tensile strength and elongation at break of the polyurethane elastomer were 1.0 MPa and 135%, respectively.

**Table 1.** The mechanical properties of the isoxazoline elastomer and the polyurethane elastomer

Energetic binder	Curing agent	Stress [MPa]	Strain [%]
T-NT	HDI	1.0	135
AUT-NT	TINO	3.0	300

The formation of the isoxazoline elastomer is shown in Figure 8. The  $-CNO$  groups react with the  $C=C$  bonds to form the isoxazoline as the crosslinking points, making the system a three-dimensional network. The network structure based on AUT-NT is more regular, so the mechanical properties of the isoxazoline elastomer are better. Because of the extra dipole-dipole interactions and strong hydrogen-bonding interactions of the urethane and the isoxazoline in the hard segments, microphase separation of the isoxazoline elastomer is enhanced compared with the conventional isoxazoline elastomer without urethane segments [43, 44]. The isoxazoline elastomer consists of soft segments and hard segments arranged alternately, and chemically linked together along a macromolecular backbone, as schematically shown in Figure 9.

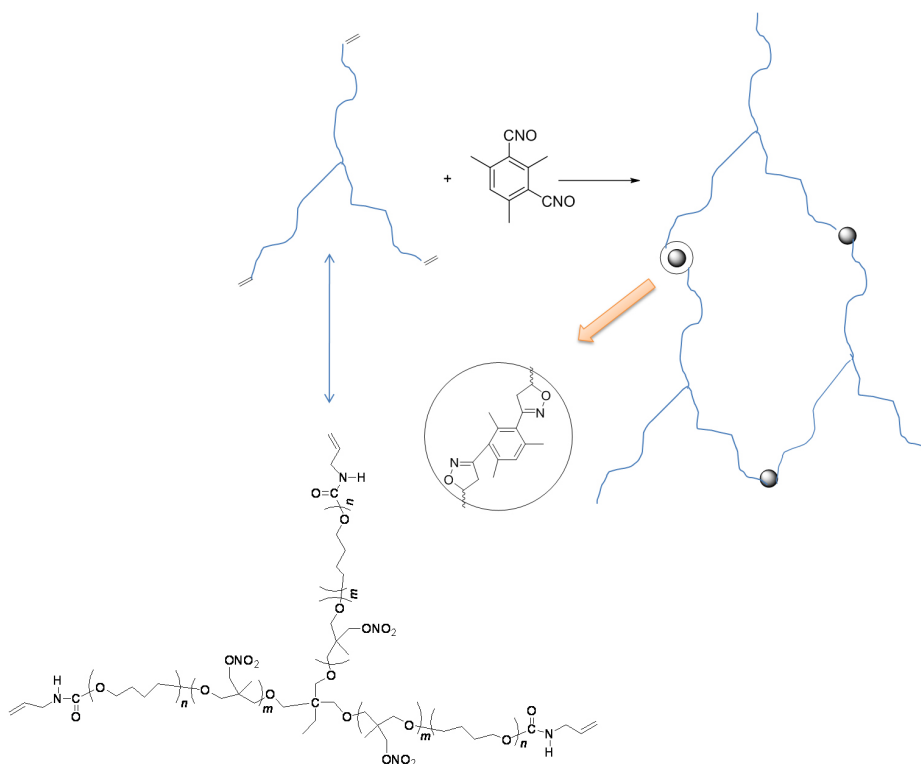


**Figure 8.** The formation of the isoxazoline elastomer

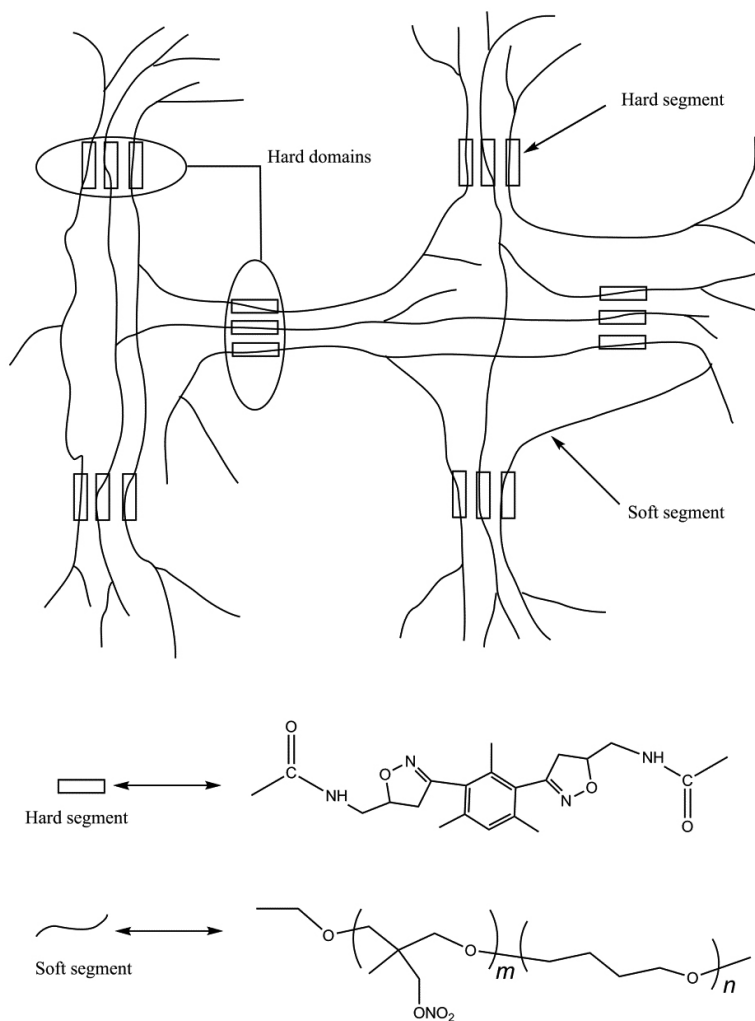


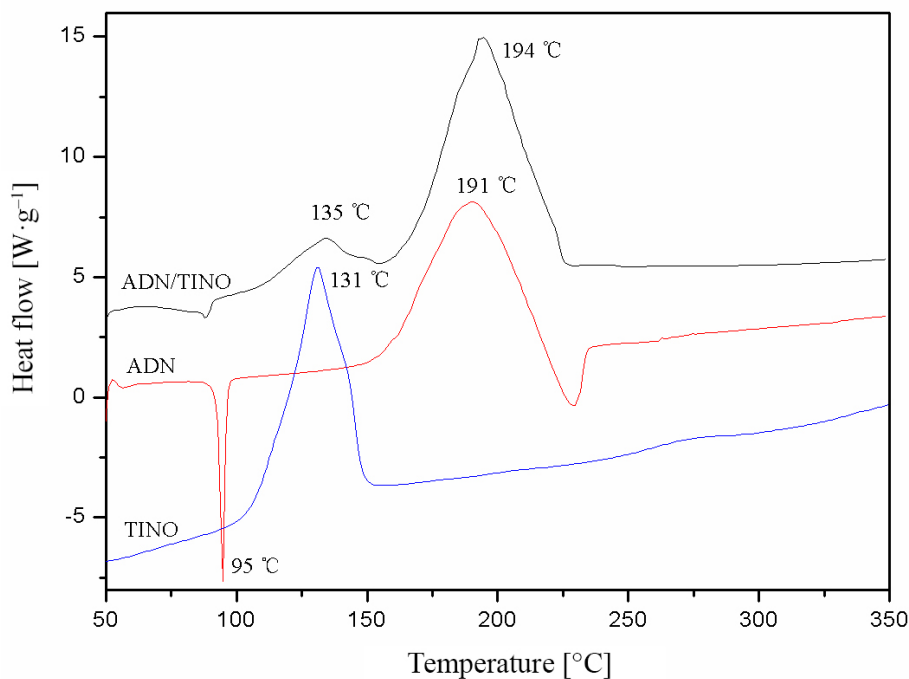
**Figure 9.** The illustration of microphase separation in the isoxazoline elastomer

The formation of microphase-separated structures arose from hard and soft segmented chemical incompatibility. The hard segments, including urethane and isoxazoline, self assembled into the hard domain. Although some hard segments are dispersed into the domains of the soft segments, the extent of microphase separation is due to thermodynamic factors. Soft domains mainly affect the elasticity of material at low temperatures. Generally, the inclusion of hard segments into the soft microphase can cause appreciable elevation of the mechanical properties of a material [45, 46].

As a result, the isoxazoline elastomer based on AUT-NT and TINO has shown improved mechanical properties compared to the polyurethane elastomer based on T-NT and HDI. The tensile strength and elongation at break of the isoxazoline elastomer were 3.0 MPa and 300%, respectively.

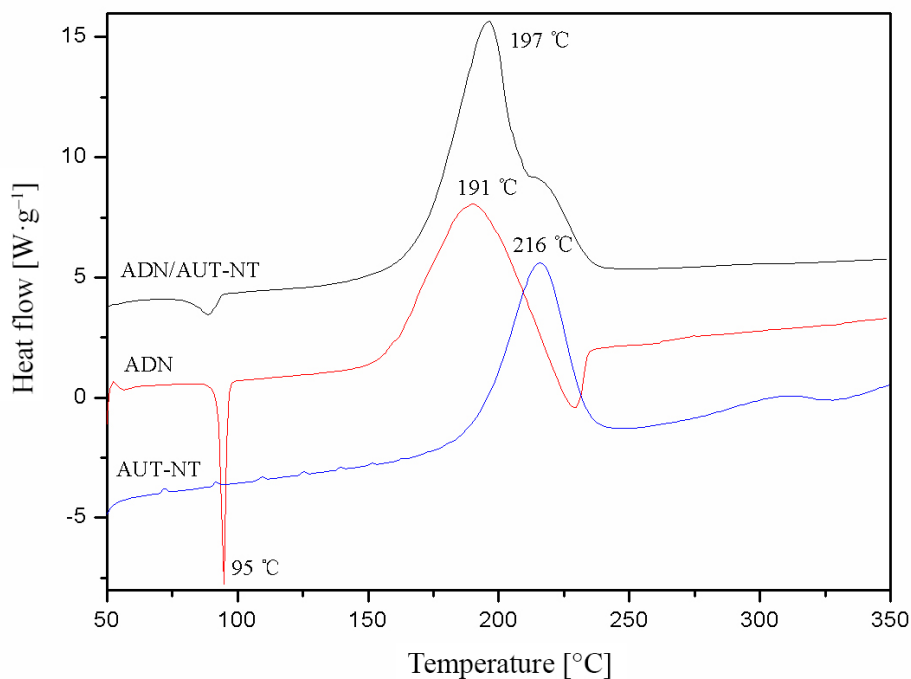
### 3.6 The compatibility of TINO and AUT-NT with energetic materials

The DSC curves of ADN, TINO/AUT-NT and their mixtures are shown in Figure 10. The respective compatibility of TINO and AUT-NT with energetic materials (HMX, RDX, CL-20, Al and ADN) was studied. Their maximum exothermic peak temperatures are shown in Table 2, and the evaluated standards of compatibility for explosive and contacted materials [14] are listed in Table 3.



(a)





(b)

**Figure 10.** DSC curves of ADN (a, b), TINO (a), AUT-NT (b) and their mixtures (a, b)

**Table 2.** Data of single and mixtures obtained by pressure DSC

Mixture system	Single system	$T_p^{1a}$ [°C]	$T_p^{2b}$ [°C]	$\Delta T_p^c$ [°C]	Rating
TINO/Al	TINO	131	133	-2	Compatible
TINO/CL-20					
TINO/RDX					
TINO/HMX					
TINO/ADN					
AUT-NT/ADN	ADN	191	197	-6	Slightly sensitized
AUT-NT/RDX	AUT-NT	216	222	-6	
AUT-NT/Al			218	-2	
AUT-NT/CL-20			212	4	
AUT-NT/HMX			HMX	284	

<sup>a</sup>  $T_p^1$  is the maximum exothermic peak temperature of a single system; <sup>b</sup>  $T_p^2$  is the maximum exothermic peak temperature of a mixture system; <sup>c</sup>  $\Delta T_p = T_p^1 - T_p^2$

**Table 3.** Data of single and mixture systems obtained by pressure DSC

$\Delta T_p$ [°C]	Rating	Note
$\leq 3$	A Compatible	Safe for use in any explosive design.
3-5	B Slightly sensitized	Safe for use in testing; not to be used as a binder material.
6-15	C Sensitized	Not recommended for use with explosive items.
$>15$	D Poorly compatibility	Hazardous. Do not use under any conditions.

From Figure 10 and Tables 2 and 3, ADN is compatible with TINO and AUT-NT. The TINO/HMX, TINO/RDX, TINO/CL-20, TINO/Al, AUT-NT/RDX, AUT-NT/ADN and AUT-NT/Al binary mixtures have good compatibility. However, the AUT-NT/HMX and AUT-NT/CL-20 binary mixtures are slightly sensitized.

## 4 Conclusions

An allyl urethane NIMMO-THF copolyether with three functional groups (AUT-NT) was synthesized from tri-functional NIMMO-THF copolyether (T-NT) and allyl isocyanate, to produce material as an energetic binder for polymer bonded explosives and solid rocket propellants. T-NT with three functional groups was synthesized by cationic ring opening polymerization of NIMMO and THF in the presence of TMP and catalyzed by  $\text{BF}_3 \cdot \text{OEt}_2$ . The structures of these polymers were confirmed by FT-IR,  $^1\text{H}$  NMR, and  $^{13}\text{C}$  NMR. Tensile testing evaluated the ultimate mechanical properties of a polyurethane elastomer based on T-NT and HDI and an isoxazoline elastomer based on AUT-NT and TINO. These showed an increase in tensile strength from 1.0 to 3.0 MPa and elongation at break from 135 to 300%, respectively. These results indicated that AUT-NT exhibited satisfactory mechanical properties, and is expected to be used in composite solid propellants and polymer bonded explosives.

## Acknowledgements

This work was supported by the National Natural Science Foundation of China (Grant No. 51373159).

## References

- [1] Krishnan, S.P.; Ayyaswamy, K.; Nayak, S.K. Hydroxy Terminated Polybutadiene: Chemical Modifications and Applications. *J. Macromol. Sci., Part A: Pure Appl. Chem.* **2013**, *50*(1): 128-138.
- [2] Haska, S.B.; Bayramli, E.; Pekel, F.; Özkar, S. Mechanical Properties of HTPB-IPDI-based Elastomers. *J. Appl. Polym. Sci.* **1997**, *64*(12): 2347-2354.
- [3] Sekkar, V.; Gopalakrishnan, S.; Ambika Devi, K. Studies on Allophanate-Urethane Networks Based on Hydroxyl Terminated Polybutadiene: Effect of Isocyanate Type on the Network Characteristics. *Eur. Polym. J.* **2003**, *39*(6): 1281-1290.
- [4] Mao, K.; Xia, M.; Luo, Y. Thermal and Mechanical Properties of Two Kinds of Hydroxyl-terminated Polyether Prepolymers and the Corresponding Polyurethane Elastomers. *J. Elastomers Plast.* **2016**, *48*(6): 546-560.
- [5] Fainleib, A.M.; Hourston, D.J.; Grigoryeva, O.P.; Shantalii, T.A.; Sergeeva, L.M., Structure Development in Aromatic Polycyanurate Networks Modified with Hydroxyl-terminated Polyethers. *Polymer* **2001**, *42*(20): 8361-8372.
- [6] Kim, H.; Lim, C.; Hong, S. Gas Permeation Properties of Organic-Inorganic Hybrid Membranes Prepared from Hydroxyl-terminated Polyether and 3-Isocyanatopropyltriethoxysilane. *J. Sol-Gel Sci. Technol.* **2005**, *36*(2): 213-221.
- [7] Selim, K.; Özkar, S.; Yilmaz, L. Thermal Characterization of Glycidyl Azide Polymer (GAP) and GAP-based Binders for Composite Propellants. *J. Appl. Polym. Sci.* **2015**, *77*(3): 538-546.
- [8] Nazare, A.N.; Asthana, S.N.; Singh, H. Glycidyl Azide Polymer (GAP) – an Energetic Component of Advanced Solid Rocket Propellants – a Review. *J. Energ. Mater.* **1992**, *10*(1): 43-63.
- [9] Kasikçi, H.; Pekel, F.; Özkar, S. Curing Characteristics of Glycidyl Azide Polymer-based Binders. *J. Appl. Polym. Sci.* **2015**, *80*(1): 65-70.
- [10] Frankel, M.B.; Grant, L.R.; Flanagan, J.E. Historical Development of Glycidyl Azide Polymer. *J. Propul. Power* **1992**, *8*(3): 560-563.
- [11] Murali Mohan, Y.; Mohana Raju, K.; Sreedhar, B. Synthesis and Characterization of Glycidyl Azide Polymer with Enhanced Azide Content. *Int. J. Polym. Mater.* **2006**, *55*(6): 441-455.
- [12] Kempa, T.J.; Barton, Z.M.; Cunliffe, A.V. Mechanism of the Thermal Degradation of Prepolymeric Poly(3-nitratomethyl-3-methyloxetane). *Polymer* **1999**, *40*(1): 65-93.
- [13] Ahmad, S.R.; Russell, D.A.; Golding, P. Laser-induced Deflagration of Unconfined HMX – the Effect of Energetic Binders. *Propellants, Explos., Pyrotech.* **2010**, *34*(6):513-519.
- [14] Liao, L.-Q.; Wei, H.-J.; Li, J.-Z.; Fan, X.-Z.; Zheng, Y.; Ji, Y.-P.; Fu, X.-L.; Zhang, Y.-J.; Liu, F.-L. Compatibility of PNIMMO with Some Energetic Materials. *J. Therm. Anal. Calorim.* **2012**, *109*(3): 1571-1576.

- [15] Shee, S.K.; Shah, P.N.; Athar, J.; Dey, A.; Soman, R.R.; Sikder, A.K.; Pawar, S.; Banerjee, S. Understanding the Compatibility of the Energetic Binder PolyNIMMO with Energetic Plasticizers: Experimental and DFT Studies. *Propellants, Explos., Pyrotech.* **2017**, *42*(2): 167-174.
- [16] Zhang, Z.; Wang, G.; Wang, Z.; Zhang, Y.; Ge, Z.; Luo, Y. Synthesis and Characterization of Novel Energetic Thermoplastic Elastomers Based on Glycidyl Azide Polymer (GAP) with Bonding Functions. *Polym. Bull.* **2015**, *72*(8): 1835-1847.
- [17] Colclough, M.E.; Desai, H.; Millar, R.W.; Paul, N.C.; Stewart, M.J.; Golding, P. Energetic Polymers as Binders in Composite Propellants and Explosives. *Polym. Adv. Technol.* **1994**, *5*(9): 554-560.
- [18] Akhavan, J.; Kronfli, E.; Waring, S.C. Energetic Polymer Subjected to High Energy Radiation. *Polymer* **2004**, *45*(7): 2119-2126.
- [19] Hsiue, H.J.; Liu, Y.L.; Chiu, Y.S. Tetrahydrofuran and 3,3-Bis(chloromethyl)oxetane Triblock Copolymers Synthesized by Two-end Living Cationic Polymerization. *J. Polym. Sci., Part A: Polym. Chem.* **1993**, *31*(13): 3371-3376.
- [20] Liu, Y.L.; Hsiue, H.J.; Chiu, Y.S. Study on Polymerization Mechanism of 3-Nitratomethyl-3'-methyloxetane and 3-Azidomethyl-3'-methyloxetane and the Synthesis of Their Respective Triblock Copolymers with Tetrahydrofuran. *J. Polym. Sci., Part A: Polym. Chem.* **1995**, *33*(10): 1067-1613.
- [21] Ahmad, N.; Khan, M.B.; Ma, X.; Ul-Haq, N. The Influence of Cross-linking/Chain Extension Structures on Mechanical Properties of HTPB-based Polyurethane Elastomers. *Arabian J. Sci. Eng.* **2014**, *39*(1): 43-51.
- [22] Hailu, K.; Guthausen, G.; Becker, W.; König, A.; Bendfeld, A.; Geissler, E. In-situ Characterization of the Cure Reaction of HTPB and IPDI by Simultaneous NMR and IR Measurements. *Polym. Test.* **2010**, *29*(4): 513-519.
- [23] Villar, L.D.; Cicaglioni, T.; Diniz, M.F.; Takahashi, M.F.K.; Rezende, L.C. Thermal Aging of HTPB/IPDI-based Polyurethane as a Function of NCO/OH Ratio. *Materials Research* **2011**, *14*(3): 372-375.
- [24] Panicker, S.S.; Ninan, K.N. Studies on Functionality Distribution of Extractable Sol from HTPB-isocyanate Gumstock. *J. Appl. Polym. Sci.* **1995**, *56*(13): 1797-1804.
- [25] Wingborg, N. Increasing the Tensile Strength of HTPB with Different Isocyanates and Chain Extenders. *Polym. Test.* **2002**, *21*(3): 283-287.
- [26] Keskin, S.; Özkar, S. Kinetics of Polyurethane Formation between Glycidyl Azide Polymer and a Triisocyanate. *J. Appl. Polym. Sci.* **2001**, *81*(4): 918-923.
- [27] Wang, X.; Li, P.; Lu, X.; Mo, H.; Xu, M.; Liu, N.; Shu, Y. Synthesis and Curing of AUT-PNIMMO with Three Functional Groups. *Polym-Korea.* **2019**, *43*(4): 503-511.
- [28] Hagen, T.H.; Jensen, T.L.; Unneberg, E.; Stenstrøm, Y.H.; Kristensen, T.E. Curing of Glycidyl Azide Polymer (GAP) Diol Using Isocyanate, Isocyanate-Free, Synchronous Dual, and Sequential Dual Curing Systems. *Propellants, Explos., Pyrotech.* **2014**, *40*(2): 275-284.

- [29] Sekkar, V.; Ambika Devi, K.; Ninan, K.N. Rheo-kinetic Evaluation on the Formation of Urethane Networks Based on Hydroxyl-terminated Polybutadiene. *J. Appl. Polym. Sci.* **2001**, *79*(10): 1869-1876.
- [30] Keicher, T.; Kuglstatler, W.; Eisele, S.; Wetzler, T.; Krause, H. Isocyanate-free Curing of Glycidyl Azide Polymer (GAP) with Bis-propargyl-succinate (II). *Propellants, Explos., Pyrotech.* **2009**, *34*(3): 210-217.
- [31] Reshmi, S.; Arunan, E.; Nair, C.P.R. Azide and Alkyne Terminated Polybutadiene Binders: Synthesis, Cross-linking, and Propellant Studies. *Ind. Eng. Chem. Res.* **2004**, *53*(43): 16612-16620.
- [32] Li, H.; Zhao, F.; Yu, Q.; Wang, B.; Lu, X. A Comparison of Triazole Cross-linked Polymers based on Poly-AMMO and GAP: Mechanical Properties and Curing Kinetics. *J. Appl. Polym. Sci.* **2016**, *133*(17): 43341.
- [33] Mohan, Y.M.; Raju, K.M. Synthesis and Characterization of HTPB-GAP Cross-linked Co-polymers. *Des. Monomers Polym.* **2005**, *8*(2): 159-175.
- [34] Yu, Z.X.; Houk, K. Intramolecular 1,3-Dipolar Ene Reactions of Nitrile Oxides Occur by Stepwise 1,1-Cycloaddition/Retro-ene Mechanisms. *J. Am. Chem. Soc.* **2003**, *125*(2): 13825-13830.
- [35] Choe, H.; Pham, T.T.; Lee, J.Y.; Latif, M.; Park, H.; Kang, Y.K.; Lee, J. Remote Stereoinductive Intramolecular Nitrile Oxide Cycloaddition: Asymmetric Total Synthesis and Structure Revision of (-)-11 $\beta$ -Hydroxycurcularin. *J. Org. Chem.* **2016**, *81*(2): 2612-2617.
- [36] Takikawa, H.; Hikita, K.; Suzuki, K. Synthesis of Highly Functionalized Isoxazoles via Base-promoted Cyclocondensation of Stable Nitrile Oxides with Active Methylene Compounds. *Synlett* **2007**, *14*(2): 2252-2256.
- [37] Kesornpun, C.; Aree, T.; Mahidol, C.; Ruchirawat, S.; Kittakoop, . Water-assisted Nitrile Oxide Cycloadditions: Synthesis of Isoxazoles and Stereoselective Syntheses of Isoxazolines and 1,2,4-Oxadiazoles. *Angew. Chem., Int. Ed.* **2016**, *55*(12): 3997-4001.
- [38] Tsyganov, D.V.; Yakubov, A.P.; Belen'kii, L.I.; Krayushkin, M.M. Synthesis and Properties of Stable Aromatic Bis(Nitrile Oxides). *Bull. Acad. Sci. USSR, Div. Chem. Sci.* **1991**, *40*(6): 1238-1243.
- [39] Huffman, B.S.; Schultz, R.A.; Schlom, P.J. Novel Reagents for Heat-activated Polymer Crosslinking. *Polym. Bull.* **2001**, *47*(2): 159-166.
- [40] Kotel'nikov, S.A.; Sukhinin, V.S.; Ermilov, A.S. Kinetics of Formation and Curing of Oligoether Urethane Allyl Ester. *Russ. J. Appl. Chem.* **2002**, *75*(3): 477-479.
- [41] Desai, H.J.; Cunliffe, A.V.; Hamid, J.; Honey, P.J.; Stewart, M.J.; Amass, A.J. Synthesis and Characterization of  $\alpha,\omega$ -Hydroxy and Nitrate Telechelic Oligomers of 3,3-(Nitratomethyl) Methyl Oxetane (NIMMO) and Glycidyl Nitrate (GLYN). *Polymer* **1996**, *37*(15): 3461-3469.
- [42] Xu, M.; Ge, Z.; Lu, X.; Mo, H.; Ji, Y.; Hu, H. Fluorinated Glycidyl Azide Polymers as Potential Energetic Binders. *RSC Adv.* **2017**, *7*(75): 47271-47278.

- [43] Li, H.; Yu, Q.; Zhao, F.; Wang, B.; Li, N. Polytriazoles Based on Alkyne Terminated Polybutadiene with and without Urethane Segments: Morphology and Properties. *J. Appl. Polym. Sci.* **2017**, *134*(32): 45178.
- [44] He, Y.; Xie, D.; Zhang, X. The Structure, Microphase-separated Morphology, and Property of Polyurethanes and Polyureas. *J. Mater. Sci.* **2014**, *49*(21): 7339-7352.
- [45] Yilgör, I.; Yilgör, E.; Wilkes, G.L. Critical Parameters in Designing Segmented Polyurethanes and Their Effect on Morphology and Properties: a Comprehensive Review. *Polymer* **2015**, *58*: A1-A36.
- [46] Wang, G.; Guo, S.; Ding, Y. Synthesis, Morphology, and Properties of Polyurethane-triazoles by Click Chemistry. *Macromol. Chem. Phys.* **2015**, *216*(18): 1894-1904.

Received: May 14, 2019

Revised: March 19, 2020

First published online: March 27, 2020